

Optimization of 3D Contrast-Enhanced Pulmonary MR Angiography in Pediatric Patients with Cardiovascular Disease

C. K. Macgowan¹, O. Al-Kwif², S-J. Yoo^{1,3}, C. J. Kellenberger⁴, G. A. Wright²

¹Medical Imaging, University of Toronto, Toronto, ON, Canada, ²Medical Biophysics, University of Toronto, Toronto, ON, Canada, ³Paediatrics, University of Toronto, Toronto, ON, Canada, ⁴Medical Imaging, University Children's Hospital, Zurich, Switzerland

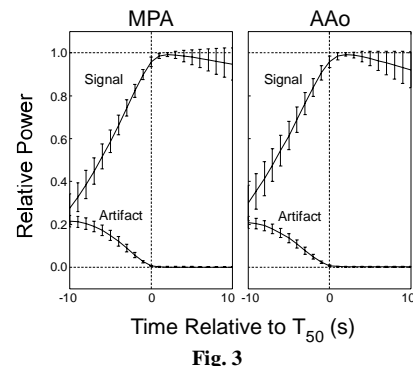
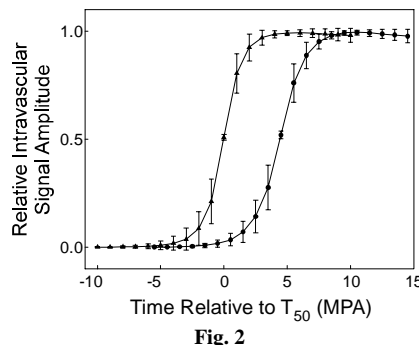
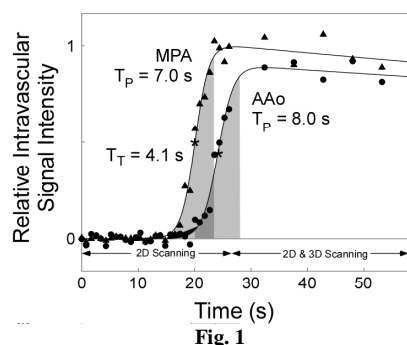
Introduction: Contrast-enhanced MRA relies on the synchronization of data acquisition to peak-contrast arrival in the target vessel. Unfortunately, test-bolus methods are not practical in small children with cardiovascular disease because the test bolus is a significant portion of the allowed contrast dose. As a result, contrast kinetics has been poorly investigated in these subjects. The goal of this work was to measure pulmonary contrast kinetics in children with cardiovascular disease during diagnostic 3D pulmonary MRA and to use this information to optimize acquisition timing.

Methods: Pulmonary MR angiographic data were collected as part of the routine diagnostic MR scanning of 12 children (age = 10.2 ± 3.5 yrs) with cardiovascular disease. Patients with known right-to-left shunts were excluded. All measurements were performed using a 1.5 T MR system (Signa CV/i, GE Health Care) and a cardiac phased-array receiver coil. A power injector (Spectris Solaris – Medrad) was used to administer 0.2 mmol/kg of gadolinium contrast medium at a flow rate of 0.044 ± 0.008 mL/s/kg followed by a 15 – 30 mL saline flush at the same rate. A previously-described fluoroscopic triggering tool was used to monitor an axial 2D slice through the main pulmonary artery (MPA), ascending aorta (AAo) and descending aorta (DAo) during contrast injection [1]. Relevant fluoroscopic imaging parameters were: imaging time = 1.4 s, matrix = 256×128 (interpolated to 512×512). Six seconds after detection of contrast in the DAo, a 3D elliptic-centric acquisition was run (scan time = 16 – 31 s). To measure contrast behavior during the 3D scan, five additional 2D axial images were acquired at equal time intervals during the 3D acquisition [2].

An ROI analysis of the fluoroscopic 2D images was performed to measure contrast signal-intensity curves in the MPA and AAo. These data were then individually fitted [3] and relevant temporal characteristics calculated (eg, see Fig. 1): time-to-peak (T_P) was defined as the time for each fit to rise from 5% to 95% of its maximum and T_T was defined as the time between the MPA and AAo fitted curves reaching 50% of their maxima (T_{50}).

A numerical simulation was performed to study how image quality related to changes in contrast-agent concentration during k-space sampling [4,5]. Each fitted curve was first normalized by its peak intensity and then resampled to simulate k-space data acquisition according to the actual elliptic-centric sampling pattern used for that subject. This analysis was repeated while varying the start of data acquisition (t_s) relative to T_{50} for each curve ($-10 \text{ s} < t_s < 10 \text{ s}$). The synthetic k-space data were then Fourier transformed to obtain the corresponding point-spread function (PSF). The signal strength and artifact (blurring and ringing) of each PSF were then quantified as functions of t_s . Signal strength was defined as the power of the central PSF peak while artifact was defined as the total power outside the central peak, both relative to the power of the central peak for $t_s = 0$ ms.

Results: Contrast-enhancement measurements from the MPA (\blacktriangle) and AAo (\bullet) of one subject are presented in Fig. 1. Values of T_P are indicated by the shaded regions while T_T corresponds to the time between the asterisks (\star) that designate T_{50} . Data from each subject were similarly analyzed and used to produce the curves shown in Fig. 2. Measured timing parameters were: $T_P(\text{MPA}) = 4.9 \pm 2.2$ s, $T_P(\text{AAo}) = 6.1 \pm 2.2$ s and $T_T = 4.5 \pm 0.6$ s.



The dependence of signal strength and artifact on the timing of data acquisition is shown in Fig. 3. Low signal and severe artifact occurred if data acquisition started well ahead of contrast arrival (i.e., $t_s \ll 0$ s). As data acquisition was delayed, contrast enhancement produced a commensurate increase in signal. Artifact power also decreased, reflecting the smaller intravascular signal variation present over the acquisition window. For both vessels, signal strength peaked weakly at $t_s = 2.3 \pm 1.4$ s. This time corresponded to 4.7 ± 2.3 s after the first arrival of contrast in the MPA and 5.6 ± 2.3 s in the AAo. Signal strength subsequently decreased as contrast cleared, while artifact was negligible during this time.

Discussion: The consistent contrast enhancement measured in these subjects suggests that high-resolution pulmonary MR angiography can be performed using a fixed acquisition protocol despite variations in weight, age, heart rate, sedation and pathology. Artifact was found to be negligible if data acquisition started at peak enhancement or later, consistent with previous studies [4,5]. Furthermore, longer delays were shown to produce only small decreases in signal strength, meaning longer acquisition delays could be used to allow greater filling of downstream vessels and to account for intra-subject timing variations. Given the multi-focal nature of congenital heart disease, imaging of the thoracic aorta and great arteries is important even if the pulmonary anatomy is primarily affected. For this reason, studies of cardiovascular disease at our institution trigger data acquisition using the AAo enhancement curve and a delay of 7.9 s. This value equals the mean AAo T_P plus one standard deviation to account for inter-subject variability (i.e., $5.6 \text{ s} + 2.3 \text{ s}$), and corresponds to approximately 6 – 7 s after peak enhancement in the MPA. By that time, signal strength in the MPA will have decreased less than 10%.

References: [1] Farb *et al.* Radiology (2001) p.244 [2] Fain *et al.* Magn Reson Med (2001) p.690 [3] Hazle *et al.* J Magn Reson Imaging (1997) p.1084 [4] Maki *et al.* J Magn Reson Imaging (1996) p.642 [5] Wilman *et al.* Magn Reson Med (2001) p.541